

SIMULATION DESIGN OF ES DEVICE USING MATLAB AND ARDUINO PLATFORMS

FARAH JALAL JASEEM*, JAMEEL KADHIM ABED AND AHMED RASHID AJEL

Department of Medical Electronic Instrumentation Engineering Techniques
Electrical Engineering Technical College
Middle Technical University

Muasker Al Rashid Street, Baghdad 10066, Iraq
{ dr_jameel57; dr_ahmed.r }@mtu.edu.iq

*Corresponding author: farahjalal503@yahoo.com

Received April 2023; accepted July 2023

ABSTRACT. *The problem of treating chronic wounds has become a critical condition for patients who suffer from chronic diseases such as diabetic foot disease, as this condition has become life-threatening for many people in the world. Electrical stimulation devices have played an important role in treating many cases and directly affected the development of therapeutic techniques and health care in the field of treatment and healing of wounds of all kinds. In this paper, the electrical stimulation device is designed by simulating the design of all the characteristics and parts of the device based on Matlab Simulink in addition to the Arduino platforms Integrated Development Environment (IDE) and fritzing. The model designed and proposed in this study provides the characteristics of current, voltage and variable frequencies. It is suitable for many medical conditions and different types of wounds, whether they are acute or chronic, by providing a direct or monophonic current signal with different strengths and variable periods that help in the healing process.*

Keywords: Matlab Simulink (MS), Integrated Development Environment (IDE), Direct Current (DC), Monophonic Current (MPC)

1. **Introduction.** Internal and external electrical currents control the internal biological electrical cellular system through the exchange between internal and external cells at the cell and organism level, which is necessary to maintain the basic physiological processes of the body in general and the skin in particular [1]. The wound healing process is attributed to one of the functions of the skin, in addition to protecting the internal organs from external damage and maintaining the internal cellular balance by producing cellular currents, which in turn assist in the wound healing process by stimulating cells to migrate to the wound site and close it [2]. When the patient suffers from a problem in the functions of the skin, this may affect the process of generating internal cellular currents, and this leads to a delay in the healing process of wounds, such as patients who suffer from chronic diseases such as diabetes mellitus and loss of growth factor [3,4]. Researchers considered the problem of chronic wounds and wound healing to be a major problem, which led most of them to develop several therapeutic methods to accelerate wound healing, such as anti-septics, antibiotic growth factors, pressurized oxygen, and bioengineered skin substitutes, and physiotherapy methods such as Electrical Stimulation (ES) and nanogenerators [5,6] as well as polymeric hydrogel membranes that act as wound dressings augment the healing process [7]. The focus of attention and attraction for the majority of researchers is the ES devices because of their great role in activating cells and assisting the migration of fibroblasts and stem cells towards the cell sites [8]. The areas of application of electrical stimulation devices differ within health care applications, and through studies, they

have had a great role in treating wounds, especially for patients who lack natural skin properties and those who suffer from chronic diseases and diabetes mellitus, as they have a great role in stimulating skin cells migration to wound sites and stimulating cells fibrous and help them spread and accelerate the healing process [9]. This paper proposes a model for simulation designing an electrical stimulation device using Matlab and Arduino simulation, encompassing various therapeutic functionalities for wound treatments.

2. Electrical Stimulation. The wound healing process is a very complex process that goes through several stages, including coagulation, cellular multiplication, proliferation and bacterial infections associated with this process [10]. If the skin is damaged, internal currents are created to help generate the four processes to speed up the healing process, but in the case of chronic disease, the skin loses the ability to perform the healing process and reduces functionality by 25% [11]. Here comes the role of ES devices that compensate for the skin functions to increase wound healing. The ES is constructed with certain properties as follows.

1) Voltage

As described in [3], the Electromotive Force (EMF) that can move charged particles when two electrodes are linked to the body is voltage (V) (ions across cell membranes in damaged tissues). The amount of voltage applied to the wound during healing can range from 1 mv to hundreds of volts per mm area of the skin.

2) Current

As mentioned in [3,12], electro-stimulation devices utilize two types of currents: Direct Current (DC) and Monophasic Pulsed Current (MPC). In wound healing, these currents are applied with polarity, with the cathode and anode charged to generate currents that mimic or enhance the disrupted internal polarized current following tissue damage. Figure 1 illustrates the DC and MPC waveforms. Based on previous studies [3,12,13], these currents can be categorized into four different types, depending on the specific wound characteristics.

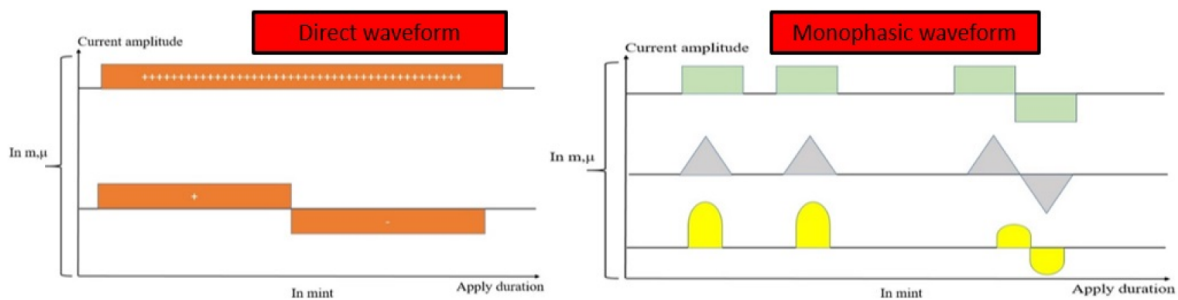


FIGURE 1. The current waveforms in the ES device

3) Method for applying the ES device

Many studies have been done within the field of using electrical stimulation devices in the treatment of wounds, but all of them agree with the principle for wound healing process as shown in Figure 2.

Several studies have explored the use of electrical stimulation devices based on the principle mentioned above. In one study [13], a conventional electrical stimulation device was utilized, resulting in increased migration of fibroblast cells in the wound area using voltage ranging from 25 to 100 mV and current ranging from 2 to 3 mA. Another study [14] focused on nanogenerators to enhance cell migration in smaller wounds, with applied currents ranging from 10 to 50 μ A. In a separate study [15], a flexible printed ES device with a gauze dressing was used to generate low voltage (4 to 40 V) and high voltage (40 to 100 V), demonstrating improved wound healing with low voltage application. In

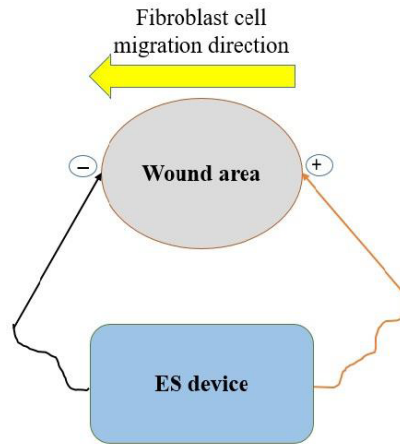


FIGURE 2. The basic principle of ES device

summary, based on the reviewed studies, electrical stimulation devices vary in therapeutic values and techniques, with voltage ranging from millivolts to over one hundred volts and current ranging from microamperes to milliamperes. This study aims to design a simulated model that accurately represents the outputs of an electrical stimulation device within these voltage and current ranges.

3. Proposal Design of ES Device. According to the principle design of the ES device as in Figure 3, the proposed design aims to design an ES device that has several characteristics and solves most of the problems facing ES devices:

- Design an easy-to-use, compact, wearable device.
- Works to save power and electrical energy by designing rechargeable outlets and power sources.
- Able to deal with different types of wounds by generating different values of current and voltage of different frequencies.

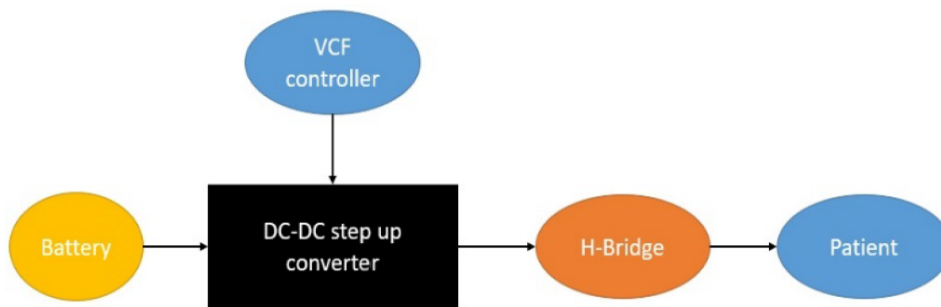


FIGURE 3. The hardware connection of ES device with patient

As in Figure 4, the ES design depends directly on the continuous voltage source, which is provided by a lithium battery, ranging in value from 3 to 3.7 volts [16]. Then the voltage output from the battery is amplified utilizing DC to DC converter [17,18], the whole system parameters voltage, current and frequency can be controlled using Arduino [19] to generate different types of signals waveform like the direct current DC and monophonic current MPC with low or high voltage intensity applying through H-bridge [20] to ensure voltage control. The stages of designing the simulation of the proposal electrical stimulation device can be divided into several stages, including the battery and the charging mechanism, voltage converting and amplification, control the voltage, current, frequency waveforms.

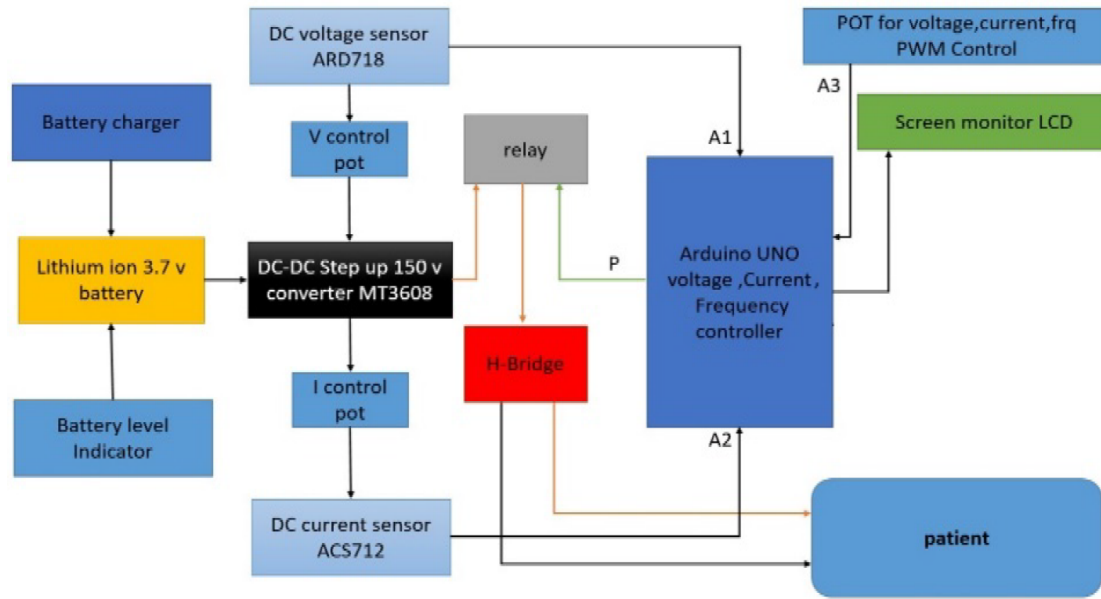


FIGURE 4. The proposed design of the ES device

4. Simulation Design and Result of ES Device. The ES device is designed using Matlab Simulink, through which necessary properties for the ES device voltage and current can be generated. The reason for using Matlab is that it gives flexibility in dealing with waves, especially in medical fields such as the brain [21], heart signals, ES, and others. The fritzing Arduino platform is used to allow ES device schematic diagram simulation and design.

4.1. Battery and charging. A lithium-ion battery with a capacity of 3.7 volts was used as the main power source. Table 1 shows the characteristics of a Li-ion battery.

TABLE 1. The Li-ion battery characteristics

Parameters	Settings
Nominal voltage	3.7 V
Rated capacity	1 Ah
Full charge voltage	4 V
The initial state of charging	95%

The charging source for the battery is represented by a secondary battery that charges the battery if the percentage of charge in the primary battery drops below 95% when the state of charge of the main battery is equal to or less than this percentage the secondary battery will work through the circuit breaker to ensure the continued provision of power to the rest of the device and to prevent interruptions.

The Matlab function block in Figure 5 will read and detect the SOC of battery 1 (B1) if it is less than or equal to 95% and the circuit breaker (BK 4 and BK 2) will be in a short circuit and discharge the battery (B2) in (B1) to reach the full charging state. The output of the charging and discharging of the battery unit is shown in Table 2 for 30 s sampling times.

4.2. DC to DC boost converter unit. In this unit, the DC voltage is enlarged to different values that are suitable for the applications to be used in the wound healing process and to make the device suitable for many applications. This unit depends on several data during the design of the boost converter as in [24]. Figure 6 illustrates the working principle and the modelling of the boost converter.

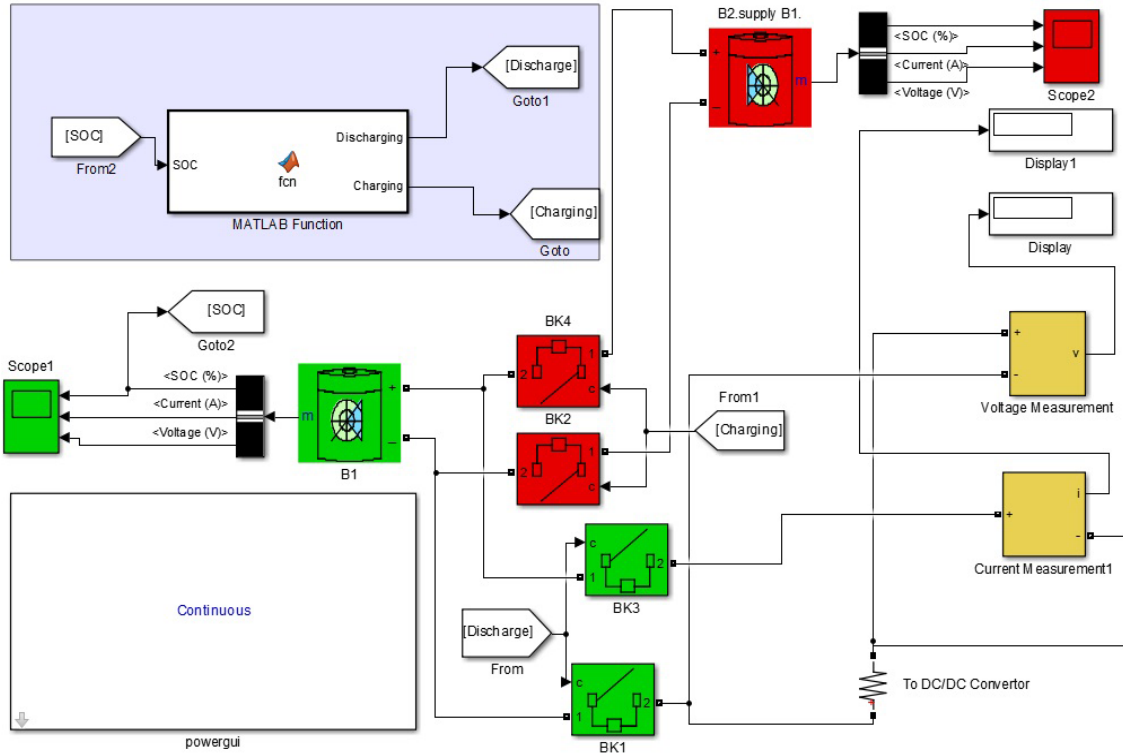


FIGURE 5. The battery and charging using Matlab

TABLE 2. The output of the battery unit

Parameters	Settings
Output voltage	3.72 V
Output current	0.52 Ah
SOC	99%

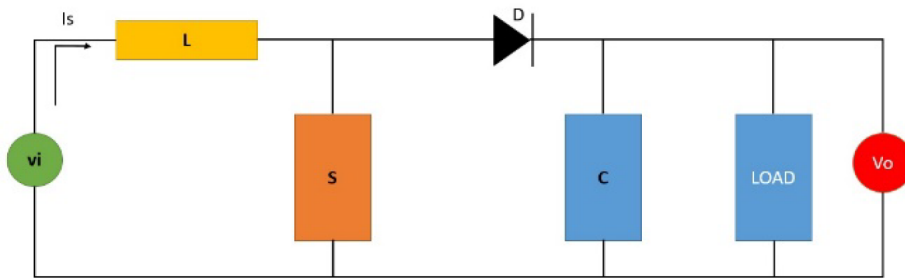


FIGURE 6. The boost converter circuit

The boost converter works based on the switches on and off modes:

- A. Switch on and Diode off.
- B. Switch off and Diode on.

The time of the duty cycle is defined as

$$T = T_{on} + T_{off} \tag{1}$$

where T_{on} is the on-time of the switch, and T_{off} is the off-time of the switch.

The switching frequency is defined as

$$F = 1/T \tag{2}$$

where T is the full-time period of Equation (1).

The duty cycle (D) is

$$D = T_{on}/T \tag{3}$$

Using the KVL for mode A to analyze the steady-state operation of the boost converter:

$$V_i = V_L \tag{4}$$

where V_i is the input voltage, and V_L is the inductor voltage.

The duty cycle will equal the T_{on} only. Again recall KVL for mode B:

$$V_i = V_o + V_L \tag{5}$$

The voltage relationships in all cases depend on the amount of voltage in the inductor, so choosing the value of the inductor in the design is very important. Figure 7 shows the Matlab Simulink of the boost converter as below.

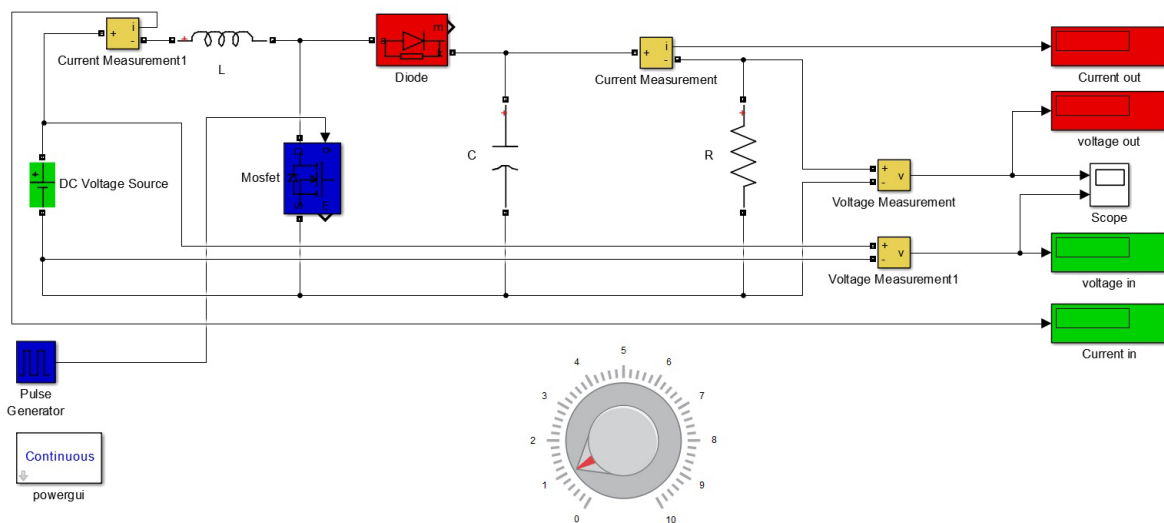


FIGURE 7. The boost converter using Matlab Simulink

In this design, a wave generator was used to control the working time of the switch for the on and off period, and a variable resistance associated with the output unit was used to control the amount of voltage and the amount of current that will be supplied to the rest of the device units as shown in Table 3.

TABLE 3. The simulation of boost convertor using Matlab

V_{in} (V)	I_{in} (A)	F_s (Hz)	L (H)	Dc	I_o (A)	V_o (V)	C (μ f)
3.7	0.5	200	0.001	95	0.85	150	33
3.7	0.5	200	0.001	60	0.36	36	33
3.7	0.5	200	0.001	40	0.18	18	33
3.7	0.5	200	0.001	10	0.03	3.5	33
3.7	0.5	200	0.001	5	0.02	2.8	33

Table 3 shows that adjusting the duty cycle in the boost converter affects the output voltage and current. With a duty cycle of 95%, the voltage can reach a maximum of 150 V and a minimum of 2.8 V. These voltage levels are well-suited for the electrical stimulation device in various wound healing applications.

In Matlab Simulink, voltage and current sensors are used as measurement units, which will later be replaced by Arduino models. The key principle involves providing a PWM signal to the solid-state switch within specific time intervals determined by the duty cycle.

4.3. Current waveform control. In this section, a simulation process was designed to generate two types of currents: Direct Current (DC) and pulsed monophasic current. These currents aim to meet the requirements of wound healing in order to enhance the device’s versatility.

The electrical stimulation device generates different types of current signals by integrating the user’s analogue input signal with the boost output signal. This integration process is facilitated by the analogue-to-digital converter with a PWM signal, as shown in Figure 8.

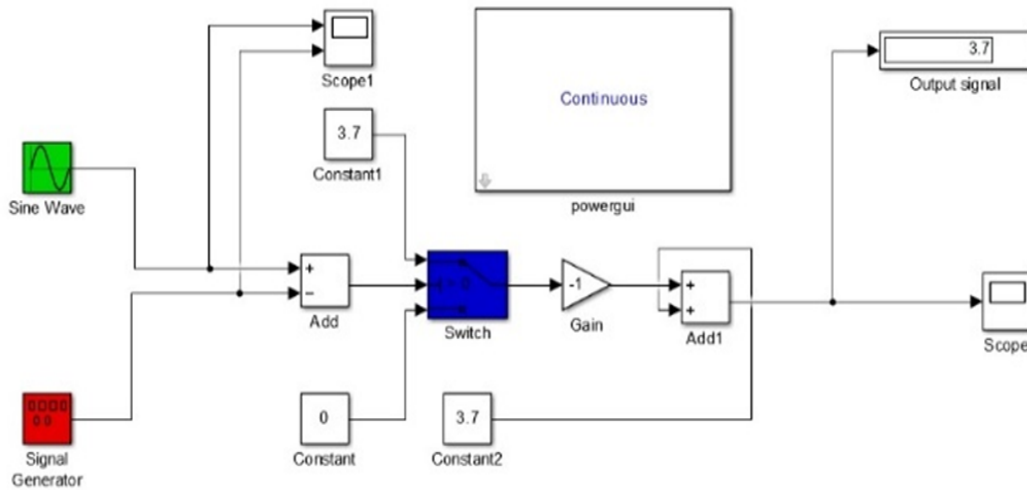


FIGURE 8. The current waveform control unit

The output of the control unit is illustrated as in Figure 9 below.

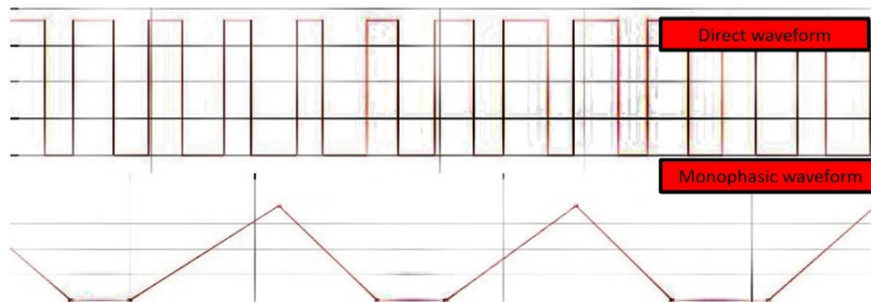


FIGURE 9. The current waveforms are produced by the control unit.

The output of the boost converter is illustrate as in Figure 10 below.

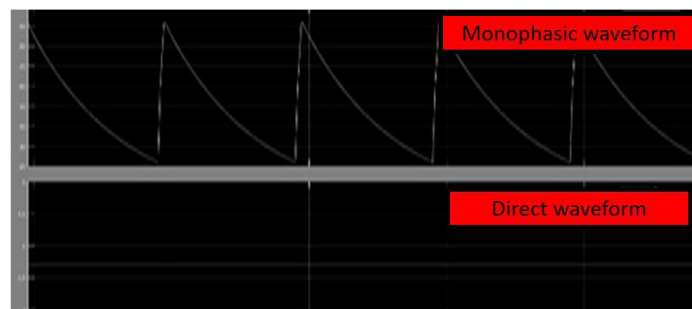


FIGURE 10. The output of the boost converter is controlled by the waveform control.

TABLE 4. The parameters of the ES using Arduino

Unit	Lable name	Function
Arduino	UNO rev3	Main controller
Relay	KY-019	Apply the voltage according to the PWM signal
H-Bridge	L298	Voltage and current driver
Boost converter	MT3608	Step up converter
Voltage sensor	ARD718	Voltage measurement
Current sensor	ACS712	Current measurement
LCD	LCD 16X2	Screen monitor
Variable resistor	R	Using A/D for selecting the treatment techniques
Battery	Li-ion	3.7 V 0.5 Ah main DC source

Perform mapping function for Equation (6):

$$y = \text{map}(X, 0, 1023, \text{value1}, \text{value2}) \tag{7}$$

where y is a new variable in digital form, value1 is the minimum value, and value2 is the maximum value.

Equation (7) can be used for any variables of the ES device based on the user selection.

5. Simulation and Control of the ES Using Arduino. In this part, the process of simulating and calibrating the outputs of the power transformer using Arduino and the available readings from the sensors based on Equations (6) and (7) as shown in Table 5 below.

TABLE 5. The control and calibration procedure

V_o of the boost	I_o of the boost	V_{sensor} (analogue)	I_{sensor} (analog)
150 V	0.85 A	1023	1023
2.8 V	0.02 A	0	0

To match the same reading the mapping Equation (7) was used based on Table 3, using the formula below:

$$V_{\text{sensor}} = \text{map}(V_o, 0, 1023, 150, 2.8) \tag{8}$$

$$I_{\text{sensor}} = \text{map}(I_o, 0, 1023, 0.85, 0.02) \tag{9}$$

The voltage-current control and selection are based on the same principle of the control and calibration procedure that perform on voltage and other variables as shown in Table 6.

TABLE 6. The voltage and current output of the L298

R1 (analogue voltage)	R2 (analog current)	V_o to relay	I_o to relay
10	12	2.8	0.024
90	84	16.8	0.082
615	620	91.2	0.41
1020	1022	146	0.78

The PWM signal of Arduino generated by the analogue signal of the R3 is used for waveform selection which will be applied to the patient through the output of the relay to select the wanted frequency by using Arduino ADC as Table 7.

Again Equation (7) can be called for different types of frequency values according to the healing techniques.

TABLE 7. The frequency generator values

Analog signal of R3	Generated PWM	Generated frequency in Hz
0	0	1
1023	255	200

6. Conclusion. ES devices have an effective impact in the field of health care because of their ability to deal with many medical applications, which include stimulation of muscles or human tissues and restoring the cellular activity of damaged or chronically diseased skin. Many studies were conducted in this field, but few of them used the methods of designing electrical stimulation devices, as most of the studies sought to study the effect of these devices on the therapeutic field and their ability to treat and heal chronic wounds. In this paper, a simulation of the electrical stimulation device was designed by the proposed model using Matlab and Arduino. The simulation results proved that the main objective of the design is to control the amount of voltage and current that is produced by the boost converter and make them different values that are suitable for most applications of the electrical stimulation device in the field of wound healing. The properties used by Arduino make it easy to control different ranges of current, voltage, and frequency to produce different shapes and values of therapeutic waves. In future work, the ES device can be implemented based on the simulation results in this research paper, and ES device monitoring technique can be used through the Internet of Things to make the device more flexible and efficient for people who are unable to move or who suffer from chronic diseases. In addition, one can enhance the present research by designing embedded systems based on FPGA to implement the classifier within real-time environment [23-36].

Acknowledgment. We are grateful to everyone we have had the pleasure of working with on this and other related issues. We would especially like to thank those who were our guides, who taught us and gave us more than we can give them credit for here.

REFERENCES

- [1] R. Fukuda et al., Mild electrical stimulation at 0.1-ms pulse width induces p53 protein phosphorylation and G2 arrest in human epithelial cells, *Journal of Biological Chemistry*, vol.288, no.22, pp.16117-16126, 2013.
- [2] M. B. Amar and M. Wu, Re-epithelialization: Advancing epithelium frontier during wound healing, *Journal of the Royal Society Interface*, vol.11, no.93, 20131038, 2014.
- [3] L. C. Kloth, Electrical stimulation technologies for wound healing, *Advances in Wound Care*, vol.3, no.2, pp.81-90, 2014.
- [4] G. Gainza, S. Villullas, J. L. Pedraz, R. M. Hernandez and M. Igartua, Advances in drug delivery systems (DDSs) to release growth factors for wound healing and skin regeneration, *Nanomedicine: Nanotechnology, Biology and Medicine*, vol.11, no.6, pp.1551-1573, 2015.
- [5] A. R. Ajel, A. Q. Al-Dujaili, Z. G. Hadi and A. J. Humaidi, Skin cancer classifier based on convolution residual neural network, *International Journal of Electrical and Computer Engineering (IJECE)*, vol.13, no.6, pp.6240-6248, DOI: 10.11591/ijece.v13i6.pp6240-6248, 2023.
- [6] R. M. Mahmood, A. R. Ajel, J. K. Abed, R. A. Mahmood, A. Al-Dujaili and A. J. Humaidi, LabVIEW-based design of smart wireless monitoring system for cardiac patients, *2023 IEEE 13th International Conference on System Engineering and Technology (ICSET)*, Shah Alam, Malaysia, pp.46-49, DOI: 10.1109/ICSET59111.2023.10295080, 2023.
- [7] E. A. Kamoun, E.-R. S. Kenawy and X. Chen, A review on polymeric hydrogel membranes for wound dressing applications: PVA-based hydrogel dressings, *Journal of Advanced Research*, vol.8, no.3, pp.217-233, 2018.
- [8] C. Chen, X. Bai, Y. Ding and I.-S. Lee, Electrical stimulation as a novel tool for regulating cell behavior in tissue engineering, *Biomaterials Research*, vol.23, no.1, pp.1-12, 2019.
- [9] G. Melotto, T. Tunprasert and J. R. Forss, The effects of electrical stimulation on diabetic ulcers of foot and lower limb: A systematic review, *International Wound Journal*, vol.19, no.7, pp.1911-1933, 2022.

- [10] A. D. J. Bombin, Electrospinning of natural polymers for the production of nanofibres for wound healing applications, *Materials Science and Engineering*, vol.114, 110994, DOI: 10.1016/j.msec.2020.110994, 2020.
- [11] S. B. Rajendran, K. Challen, K. L. Wright and J. G. Hardy, Electrical stimulation to enhance wound healing, *Journal of Functional Biomaterials*, vol.12, no.2, 40, 2021.
- [12] A. Sebastian, S. A. Iqbal, J. Colthurst, S. W. Volk and A. Bayat, Electrical stimulation enhances epidermal proliferation in human cutaneous wounds by modulating p53-SIVA1 interaction, *Journal of Investigative Dermatology*, vol.135, no.4, pp.1166-1174, 2015.
- [13] S. Snyder, C. DeJulius and R. K. Willits, Electrical stimulation increases random migration of human dermal fibroblasts, *Annals of Biomedical Engineering*, vol.45, no.9, pp.2049-2060, 2017.
- [14] W. Hu et al., Enhancing proliferation and migration of fibroblast cells by electric stimulation based on triboelectric nanogenerator, *Nano Energy*, vol.57, pp.600-607, 2019.
- [15] X.-F. Wang et al., Flexible electrical stimulation device with Chitosan-Vaseline® dressing accelerates wound healing in diabetes, *Bioactive Materials*, vol.6, no.1, pp.230-243, 2021.
- [16] Y. Feng et al., Challenges and advances in wide-temperature rechargeable lithium batteries, *Energy & Environmental Science*, vol.15, no.5, pp.1711-1759, 2022.
- [17] Y. U. Maheswari, A. Amudha, L. A. Kumar, K. Nagasaravanan, M. Sundaram and Y. Dhayanewaran, Simulation and measurement of conducted emission in DC-DC convertor, *Journal of Physics: Conference Series*, vol.1916, no.1, 012135, 2021.
- [18] R. Abhishek, P. Zoting and P. Ragit, Design and analysis of a DC-DC buck converter and boost converter to achieve high efficiency by altering duty cycle and input voltage, *International Journal of Scientific and Research Publications (IJSRP)*, vol.10, no.6, pp.731-738, 2020.
- [19] H. K. Kondaveeti, N. K. Kumaravelu, S. D. Vanambathina, S. E. Mathe and S. Vappangi, A systematic literature review on prototyping with Arduino: Applications, challenges, advantages, and limitations, *Computer Science Review*, vol.40, 100364, 2021.
- [20] A. I. Elsanabary, G. Konstantinou, S. Mekhilef, C. D. Townsend, M. Seyedmahmoudian and A. Stojcevski, Medium voltage large-scale grid-connected photovoltaic systems using cascaded H-bridge and modular multilevel converters: A review, *IEEE Access*, vol.8, pp.223686-223699, 2020.
- [21] M. J. Mohammed, J. K. Abed and A. J. Mahdi, Simulation of EEG-based apparatus control for quadriplegic patients, *IOP Conference Series: Materials Science and Engineering*, vol.1067, no.1, 012135, 2021.
- [22] A. Fathah, *Design of a Boost Converter*, Bachelor Thesis, Electrical Engineering, National Institute of Technology, Odisha, India, 2013.
- [23] A. R. Nasser, A. M. Hasan and A. J. Humaidi, DL-AMDet: Deep learning-based malware detector for android, *Intelligent Systems with Applications*, vol.21, 200318, pp.1-10, <https://doi.org/10.1016/j.iswa.2023.200318>, 2024.
- [24] J. Abdulhadi, A. Al-Dujaili, A. J. Humaidi and M. A. Fadhel, Human nail disease classification based on transfer learning, *ICIC Express Letters*, vol.15, no.12, pp.1271-1282, DOI: 10.24507/icicel.15.12.1271, 2021.
- [25] M. L. Muhammed, E. H. Flaieh and A. J. Humaidi, Embedded system design of path planning for planar manipulator based on chaos A* algorithm with known-obstacle environment, *Journal of Engineering Science and Technology*, vol.17, no.6, pp.4047-4064, 2022.
- [26] A. J. Humaidi, M. A. Fadhel and A. R. Ajel, Lane detection system for day vision using altera DE2, *Telkomnika*, vol.17, no.1, pp.349-361, DOI: 10.12928/TELKOMNIKA.v17i1.10071, 2019.
- [27] A. J. Humaidi, T. M. Kadhim, S. Hasan, I. K. Ibraheem and A. T. Azar, A generic Izhikevich-modelled FPGA-realized architecture: A case study of printed English letter recognition, *2020 24th International Conference on System Theory, Control and Computing (ICSTCC)*, Sinaia, Romania, pp.825-830, DOI: 10.1109/ICSTCC50638.2020.9259707, 2020.
- [28] A. J. Humaidi and T. M. Kadhim, Spiking versus traditional neural networks for character recognition on FPGA platform, *Journal of Telecommunication, Electronic and Computer Engineering*, vol.10, no.3, pp.109-115, 2018.
- [29] A. J. Humaidi, S. Hasan and M. A. Fadhel, FPGA-based lane-detection architecture for autonomous vehicles: A real-time design and development, *Asia Life Sciences*, vol.1, pp.223-237, 2018.
- [30] A. J. Humaidi, S. Hasan and M. A. Fadhel, Rapidly-fabricated nightly-detected lane system: An FPGA implemented architecture, *Asia Life Sciences*, vol.1, pp.343-355, 2018.
- [31] M. L. Muhammed, A. J. Humaidi and E. H. Flaieh, A comparison study and real-time implementation of path planning of two arm planar manipulator based on graph search algorithms in obstacle environment, *ICIC Express Letters*, vol.17, no.1, pp.61-72, DOI: 10.24507/icicel.17.01.61, 2023.

- [32] T. Ghanim, A. R. Ajel and A. J. Humaidi, Optimal fuzzy logic control for temperature control based on social spider optimization, *IOP Conference Series: Materials Science and Engineering*, vol.745, no.1, 012099, 2020.
- [33] A. J. Humaidi and M. R. Hameed, Design and performance investigation of block-backstepping algorithms for ball and arc system, *2017 IEEE International Conference on Power, Control, Signals and Instrumentation Engineering (ICPCSI)*, Chennai, India, pp.325-332, DOI: 10.1109/ICPCSI.2017.8392309, 2017.
- [34] A. J. Humaidi, A. H. Hameed and M. R. Hameed, Robust adaptive speed control for DC motor using novel weighted E-modified MRAC, *2017 IEEE International Conference on Power, Control, Signals and Instrumentation Engineering (ICPCSI)*, Chennai, India, pp.313-319, DOI: 10.1109/ICPCSI.2017.8392302, 2017.
- [35] A. J. Humaidi, S. K. Kadhim, M. E. Sadiq, S. J. Abbas, A. Q. Al-Dujaili and A. R. Ajel, Design of optimal sliding mode control of PAM-actuated hanging mass, *ICIC Express Letters*, vol.16, no.11, pp.1193-1204, DOI: 10.24507/icicel.16.11.1193, 2022.
- [36] A. R. Ajel, H. M. Abdul Abbas and M. J. Mnati, Position and speed optimization of servo motor control through FPGA, *International Journal of Electrical and Computer Engineering*, vol.11, no.1, pp.319-327, DOI: 10.11591/ijece.v11i1, 2021.
- [37] R. F. Hassan, A. R. Ajel, S. A. Jabbar and A. J. Humaidi, FPGA based HIL co-simulation of 2DOF-PID controller tuned by PSO optimization algorithm, *ICIC Express Letters*, vol.16, no.12, pp.1269-1278, DOI: 10.24507/icicel.16.12.1269, 2022.